AIAA JOURNAL
Vol. 42, No. 12, December 2004

Non-Gaussian Statistics of Atmospheric Turbulence and Related Effects on Aircraft Loads

J. G. Jones*
Stirling Dynamics, Ltd., Bristol, England BS8 1PG, United Kingdom
G. H. Watson†
QinetiQ, Ltd., Farnborough, England GU14 0LX, United Kingdom
and
G. W. Foster‡
QinetiQ, Ltd., Thurleigh, England MK44 2FQ, United Kingdom

Non-Gaussian statistical properties of turbulence in the inertial range can be characterized in terms of an exponent (k) that defines the scaling of velocity increments together with a fractal dimension (D) that quantifies "intermittency." A new method of data analysis, for measuring k and D, is presented based on the collapsing of appropriately normalized probability distributions measured at different scales. The method is illustrated by its application to records of turbulence measured at low altitudes by a specially instrumented Gnat trainer aircraft. The resulting "multifractal" statistical description of velocity increments is consistent with results obtained by previous authors using a different method of analysis, based on the scaling of velocity structure functions, and with the predictions of recent theoretical models of physical processes in the inertial range. It is demonstrated how the results can be applied directly to the estimation of aircraft loads, using a new multifractal formulation of statistical-discrete-gust theory. Qualitative differences between the resulting estimated loads and the loads predicted by the statistical method prescribed in the current airworthiness regulations, the power-spectral-density method, are identified.

I. Introduction

MEASURED wind fluctuations in the atmosphere exhibit a high degree of unpredictability, leading to the need for statistical methods to estimate associated aircraft loads. In current practice there is widespread use of a method based on Gaussian random-process theory, the power-spectral-density (PSD) method,[1–3] to estimate structural loads and other response quantities. A feature of this statistical approach is the assumption that, in terms of their effects on aircraft loads, the most significant wind fluctuations lie within the "inertial range" of scales, where the power spectral density is proportional approximately to (spatial frequency)$^{-\frac{5}{3}}$.

On the other hand, evidence exists that turbulence can exhibit a high degree of order, or structure, with turbulence velocities showing significant deviations from Gaussian statistics. As was demonstrated as early as 1972 by Chen,[4] the validity of the basic equation, due to Rice,[5] used in the PSD method to predict the statistics of aircraft loads depends heavily on the assumption that, at least in turbulence patches of limited extent, the two-point difference

$$\Delta u(y, L) = u(y + L/2) - u(y - L/2) \tag{1}$$

of a velocity component $u(y)$ over a distance L obeys approximately normal or Gaussian statistics. However, as illustrated by Chen[4] using measurements from four independent data sources, even over patches of limited extent the probability distributions of Δu in inertial-range turbulence are typically strongly non-Gaussian, as indicated by strong tails with deviations from Gaussian statistics quantified by large values of kurtosis.

Further evidence for the significance of the velocity difference Δu, Eq. (1), for aircraft loads is provided by the statistical-discrete-gust (SDG) method[6] of loads prediction, in which velocity differences are represented explicitly in the form of ramp gust components covering a range of differencing intervals, or gust-gradient distances, L, and non-Gaussian statistics are introduced in the form of distributions of exponential type to represent the velocity differences. This method exploits the fact that, in the case of response quantities with a high-pass property, that is, in which low frequencies in response are strongly attenuated, it is changes in the magnitude of the input, over an interval that "tunes" with the characteristics of response, that cause significant response magnitudes, rather than the amplitudes of the input itself.

As will be reviewed in Sec. II, non-Gaussian statistical properties of turbulence in the inertial range can be characterized in terms of an exponent (k), which defines the scaling of velocity increments, together with a fractal dimension (D) that quantifies "intermittency." As documented by Frisch,[7] a further non-Gaussian property of turbulence velocity increments is that of skewness, as reflected in odd-order moments of the probability distribution. However, this paper is concerned entirely with the statistics of the absolute value of velocity increments and the related statistics of aircraft loads.

In Sec. III, a new method of data analysis is presented for measuring k and D based on the collapsing, over limited ranges of amplitude, of probability distributions of velocity increments measured at different scales. The amplitudes of velocity increments are quantified by a nondimensional moment-order parameter p, resulting in measured functions $k(p)$ and $D(p)$. Over limited ranges of amplitude, absolute values of velocity increments are represented statistically by exponential distributions, each parameterized by a single value of p. Over larger ranges of amplitudes, corresponding to a range of values of p, the resulting distributions are of stretched exponential type[7] and can be defined as the envelope of the local exponentials. The method is illustrated by its application to records of turbulence measured at low altitudes by a specially instrumented Gnat trainer aircraft. The resulting p-dependent

Received 9 December 2002; accepted for publication 13 April 2004.

*Consultant, Clifton.
†Research Engineer, Guidance and Imaging Solutions, Farnborough, Hants.
‡Capability Leader for Weapon Aerodynamics, Aerodynamics Integration Group, Building 109, Thurleigh, Bedford.

multifractal statistical description of velocity increments will be shown to be consistent qualitatively with results obtained by previous authors using a different method of data analysis, based on the scaling of velocity structure functions, and with the predictions of a recent theoretical model of physical processes in the inertial range. However, it will be demonstrated that the method of analysis described here has the advantage, for aeronautical applications, of exploiting the influence of $k(p)$ and $D(p)$ on the probability distributions of the outputs of responding systems, where the "system" may be either a data-processing filter or an aircraft structural load. These results are achieved in terms of a new multifractal formulation of statistical-discrete-gust (SDG) theory.[6] By this means, the probability distributions of load amplitudes are related to an associated multifractal distribution of velocity increments.

II. Scaling Exponents: Background

A. Introduction

Basic concepts in the theory of atmospheric turbulence were introduced in two seminal papers published, respectively, in 1941 and 1962 by Kolmogorov,[8,9] commonly referred to as the K41 and K62 papers. Both of these papers concern the probabilities of observing different possible values of Δu, Eq. (1). In the K41 or classical theory[8] of high-Reynolds-number turbulence in the inertial range, a scale symmetry is assumed in the form of global dilational invariance, or self-similarity. In this classical theory, the power-spectral density follows a $(-\frac{5}{3})$ power law and the probability distribution of the normalized difference $\Delta u(y, L)/L^k$, Eq. (1), becomes independent of L when the scaling exponent k takes the value $\frac{1}{3}$.

However, deficiencies in this "self-similar" model were discussed in the K62 paper by Kolmogorov[9] and also by Obukhov.[10] Subsequently the kurtosis of two-point velocity differences in the inertial range was shown experimentally[11,12] not to be scale-invariant, as required by the classical K41 theory, but to increase with decreasing separation L. Large values of the kurtosis of velocity differences imply the existence of relatively large differences embedded in families of small differences (regions of low turbulence activity). Thus an associated result is that turbulence was found to be intermittent, the intermittency being most pronounced at very small scales.[7]

To account for the observed intermittency, Mandelbrot (1974)[13] and others (Frisch et al., 1978[14]) introduced statistical models in which singularities in velocity gradient are concentrated in sets, or regions, having noninteger, or fractal, dimension $\boldsymbol{D}$. In these models fluctuations in $\Delta u(y, L)$, Eq. (1), are active only in sets of points having fractal dimension $\boldsymbol{D} < 3$, whereas for a Gaussian process $\boldsymbol{D} = 3$.

Subsequently, this representation was refined by the introduction[15–17] of nested sets where the strengths of the singularities vary between sets, the so-called "multifractals." On each such set, the normalized velocity difference $\Delta u(y, L)/L^k$ becomes independent of L when a value of the scaling exponent k is chosen appropriate to that set, k being smaller for sets carrying fluctuations of higher intensity. Results of laboratory measurements were shown to be broadly consistent with such multifractal statistical models.[17] Reviews of these topics, in the form that existed in 1991, were given by Meneveau and Sreenivasan[18] and by She et al.[19]

In 1988 a review was presented by Jones et al.[20] of applications of the above concepts made over the previous 10 years, at the (U.K.) Royal Aircraft Establishment, to aircraft load prediction. There it was shown, in particular, how loads predicted by the beta model of Frisch et al.[14] differed from those predicted by a self-similar model consistent with Kolmogorov's original (K41) theory.[8]

B. Scaling Exponents and Probability Distributions

One approach to the measurement of scaling exponents, first outlined in Ref. 20 and the basis of the new method of data analysis to be described in Sec. III, involves the collapsing of appropriately normalized probability distributions measured at different scales. In this method, two-point velocity differences $\Delta u(y, L)$, Eq. (1), are evaluated for different distances L. However, to make a valid comparison of measurements of Δu at different scales, allowance must be made for the loss of information at the smallest scales arising from the sampled nature of measured data. In particular, the two-point differences $\Delta u(y, L)$ associated with values of L on the order of the sampling interval contain no contribution from fluctuations of scale less than L (such high-frequency fluctuations having been removed by analog antialiasing filters prior to sampling). To achieve a valid comparison between small and large scales the data are therefore smoothed numerically on each of the larger scales L before differences are taken, so that contributions from scales less than L are removed consistently. Subsequent analysis is thus based upon the smoothed-difference function

$$\overline{\Delta u}(y, L) = \int H(x - y, L)\Delta u(x, L)\,\mathrm{d}x \tag{2}$$

where the weighting factor $H(x, L)$ is a smoothing function (low-pass filter) that introduces a local average over a distance of order L.

Scaling properties of velocity differences are derived from measured local extreme values of $\overline{\Delta u}(y, L)$, Eq. (2), with respect to y at each of a set of prescribed values of scale L. Specifically, for each such value of L, a cumulative distribution $n(L, X)$ is defined as the average number, per unit distance y, of local extrema in the function $\overline{\Delta u}(y, L)$ having magnitude greater than X. Scaling exponents are then introduced that enable $n(L, X)$ to be expressed as a scale-invariant function of X. Such distributions, and associated scaling exponents, may be obtained for the absolute value of velocity increments, as is done in this paper, or for positive and negative increments considered separately.

To express $n(L, X)$ in scale-invariant form it is necessary to introduce the fractal dimension D of one-dimensional intersections of the flow field: in the fractal representation, $L^D n(L, X)$ becomes a scale-invariant function of X/L^k, where D and k are related exponents. D was related by Mandelbrot[13] to the fractal dimension $\boldsymbol{D}$, which refers to properties of fluctuations in a three-dimensional flow field, by the equation

$$D = \boldsymbol{D} - 2 \tag{3}$$

although recent work[21] has questioned this simple relationship, showing by a detailed analysis of measured turbulence data that significant departures from this equation can arise as a consequence of nonfractal inclusions in an otherwise fractal background structure.

Frisch[7] refers to experimental evidence[11,22,23] that the tails of probability distributions of velocity increments in turbulence decay in a roughly exponential manner. Further support for the use of exponential distributions as applied to turbulence velocity differences and derivatives is provided by Narasimha.[24] Assuming an exponential model, the dependence of $L^D n(L, X)$ on X/L^k takes the form

$$L^D[n(L, X)] = \alpha \exp(-X/\beta L^k) \tag{4}$$

In a preliminary analysis[20] of a subset of the measurements analyzed in this article, plots of $L^D n(L, X)$ as functions of X/L^k were presented for selected individual runs. These showed that, except at the lowest fluctuation amplitudes, as compared with a self-similar model with $D = 1$ and $k = \frac{1}{3}$ (which would be consistent with the Kolmogorov K41 theory[8]), improved overall fits to the data were achieved with empirically determined values with $D < 1$ and $k < \frac{1}{3}$. Subsequent analysis[25] of a larger data set showed that different pairs of values of D and k caused $L^D n(L, X)$ to become a scale-invariant function of X/L^k over different ranges of amplitude.

To provide a rigorous quantitative basis for this qualitative trend, it is shown in Sec. III how an independent nondimensional measure of fluctuation amplitude can be defined in the form of a moment-order parameter p and amplitude-dependent exponents $D(p)$ and $k(p)$ derived from measured probability distributions in the form of functions of p.

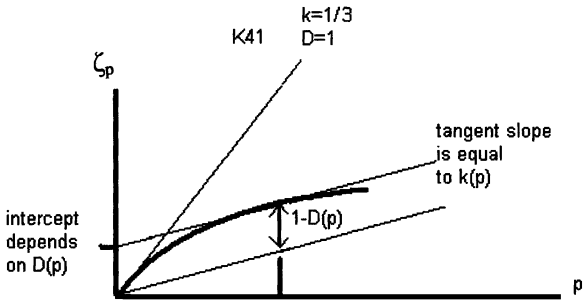

Fig. 1 Structure-function scaling exponent ζ_p. Based on the Legendre transformation, each tangent, parameterized by p, is specified by a slope $k(p)$ and an intercept determined by $D(p)$. ζ_p is the envelope of these tangents.

C. Scaling Exponents and Structure Functions

In contrast to the derivation of scaling exponents from measured probability distributions, outlined above, most previous work on scaling exponents, both experimental and theoretical, has been based on the so-called "structure functions," which define the moments of velocity differences, Eq. (1). The structure function of order p is defined, in the terminology of Eq. (1), by

$$S_p(L) = \langle (\Delta u(L))^p \rangle \tag{5}$$

(where the variable y has been dropped to ease notation).

In the case of the Kolmogorov K41 theory,[8] in which the scaling exponent for velocity differences is given by $k = \frac{1}{3}$, it follows that $S_p(L) \propto L^{p/3}$. More generally, experimental work on intermittency in the inertial range[7] suggested that structure functions follow power laws of the form

$$S_p(L) \propto L^{\zeta_p} \tag{6}$$

where the ζ_p are called the exponents of structure functions. Thus in the K41 theory $\zeta_p = p/3$. In the case of the beta model of Frisch et al.[14] the exponents take the theoretical value $\zeta_p = p/3 + (3 - \boldsymbol{D})(1 - p/3)$, reducing to the K41 value when the fractal dimension $\boldsymbol{D} = 3$.

Experimental results,[12,26] however, showed ζ_p to be a nonlinear function of p, concave downward as illustrated qualitatively in Fig. 1. This led Parisi and Frisch[15] to develop the multifractal model, in which the turbulent flow is assumed to possess a continuous range of scaling exponents k, with each value of which a fractal dimension $\boldsymbol{D}(k)$ is associated. As described in Ref. 7, the structure function $S_p(L)$ may then be expressed as an integral over the range of scaling exponents. Application of the approximate method of steepest descent then allows[7] a model defined in terms of the set of measured structure function exponents ζ_p to be interpreted as a multifractal model through a relationship, illustrated in Fig. 1, in which, for each value of p, k is given by the slope of the tangent to the curve $\zeta_p(p)$ and D [assumed to be related to $\boldsymbol{D}$ through Eq. (3)] is defined by the offset of this tangent from a parallel line through the origin. As explained in Ref. 7 this relationship between the dimension D, k, and the exponents ζ_p may be derived from a Legendre transformation.

In 1991 She et al.[19] presented a review of results on homogeneous turbulence, both experimental and theoretical, covering the period from the Kolmogorov K41 theory[8] to the subsequent multifractal theories.[15–17] Subsequently, considerable effort has been directed to explaining the nonlinear dependence of ζ_p on p and associated variations in the functions $k(p)$ and $D(p)$, illustrated qualitatively in Fig. 1, in terms of theoretical models and the underlying physics.[27–34] In particular, She and Leveque[28] proposed a phenomenological model in which the statistical picture of multifractal turbulence is reconciled with a geometric picture based on vortex filaments. This model predicted a specific form for the $\zeta_p(p)$ curve illustrated in Fig. 1:

$$\zeta_p = p/9 + 2 - 2\left(\tfrac{2}{3}\right)^{p/3} \tag{7}$$

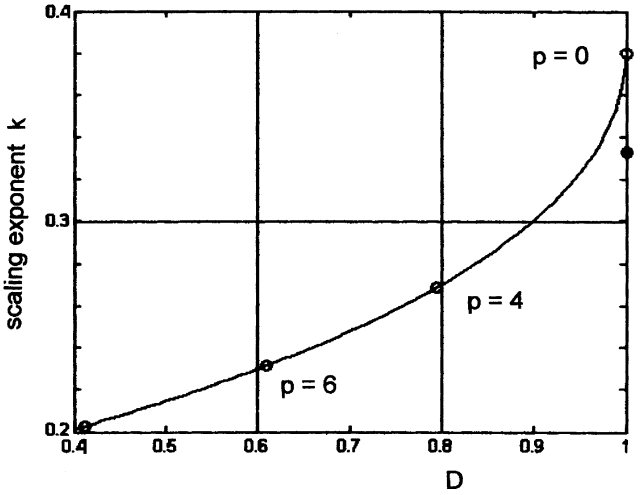

Fig. 2 Scaling exponents $k(p)$ and $D(p)$ from model of She and Leveque,[28] Eq. (7). Circled points correspond to $p = 0$, 4, 6, and 8. Also shown is data point $D = 1$, $k = \frac{1}{3}$, corresponding to K41 model.

which was shown[28] to be in very good agreement with experimental values obtained for longitudinal structure functions. Using the relationship illustrated in Fig. 1, Eq. (7) implies a $D(k)$ relationship (Fig. 2) in which $D(\frac{1}{3}) = 0.97$, $D(0.381) = 1$, and $k_{\min} = \frac{1}{9}$.

III. Scaling Exponents: New Method of Data Analysis

Although most previous measured estimates of the multifractal scaling exponents $k(p)$ and $D(p)$ have been derived indirectly from measured structure-function exponents via the Legendre transformation, as illustrated in Fig. 1, the possibility was referred to by Frisch[7] of measuring these exponents directly in terms of the probability density function of velocity increments. In this context Frisch introduced[7] a probabilistic reformulation of the multifractal model which avoids the assumption, adopted in the original multifractal model as defined by Parisi and Frisch,[15] that $D(p)$ is the fractal dimension of a singular set and has, moreover, the further advantage of allowing exponents for positive and negative velocity increments to be measured independently. For our purposes, as we shall demonstrate, this approach has the added advantage of providing a direct bridge to the probability distributions of aircraft loads, in a form with which loads engineers are familiar.

Suppose that fluctuations in $\overline{\Delta u}(y, L)$ of amplitude X have a probability density function $f(X)$, whose pth moment is given by $\int f(X)X^p \, dX$. Let X_p denote the amplitude at which $f(X)$ makes its greatest contribution to the pth moment, i.e., at which the product $f(X)X^p$ is greatest. The resulting stationarity condition

$$X_p = -p[f(X)/f'(X)]_{X_p} \tag{8}$$

provides a means of labeling the amplitude in terms of p.

In terms of the measured number $n(L, X)$, per unit distance y, of local extrema in $\overline{\Delta u}(y, L)$ having magnitude greater than X, we make the assumption that an exponential model of the form

$$n(X) = a \exp(-X/b) \tag{9}$$

can be fitted locally, over limited ranges of amplitude X. Thus we assume that a and b, in Eq. (9), vary sufficiently slowly with X so that they may be regarded as constants within each local range. Although in this paper the method is applied to the absolute values of extrema in $\overline{\Delta u}(y, L)$, it is equally applicable when extrema corresponding to positive and negative velocity increments are modeled as separate families.

An advantage of the exponential model, Eq. (9), is that moments of all orders exist. Using Eq. (8), it is shown in the Appendix that the excess rate $n(X)$, modeled by Eq. (9), can be expressed

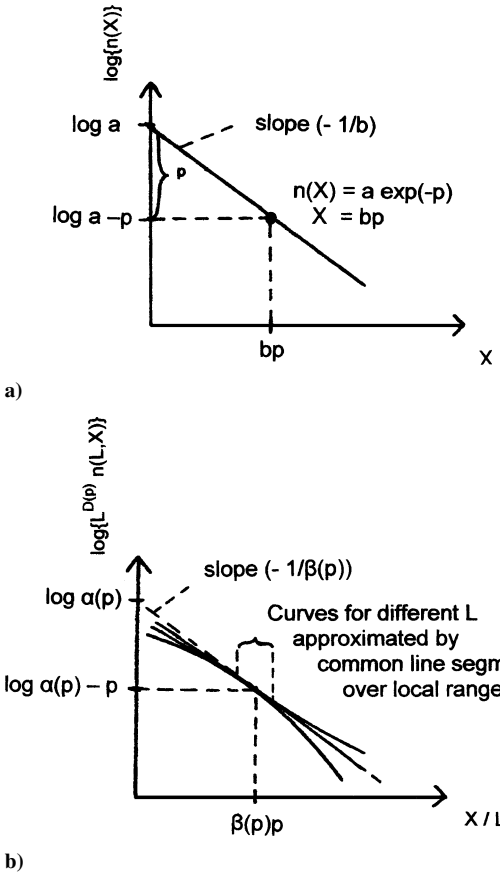

Fig. 3 Basis of method used to derive $D(p)$ and $k(p)$: a) illustration of independent variables p, a, and b and b) illustration of scale invariance over range of amplitudes centered on a value making maximum contribution to the pth moment.

parametrically in terms of the associated moment order p by the pair of equations

$$n(X) = a\exp(-p) \tag{10}$$

$$X = bp \tag{11}$$

For the purpose of deriving amplitude-dependent scaling exponents from $\overline{\Delta u}(y, L)$, the significance of the preceding implicit form for the relationship between $n(X)$ and X is that the amplitude variable p is independent of a and b. This is illustrated in a straight-line plot (Fig. 3a) of log $n(X)$ against X, in which changes in a, for fixed b, cause a vertical translation of the line, whereas changes in b, for fixed a, cause a rotation about a fixed pivot at $X = 0$ associated with a stretch of the horizontal axis. Both of these transformations leave the value of p (illustrated) unaltered.

Thus, generalizing Eqs. (10) and (11), the monofractal model defined by Eq. (4) can be expressed parametrically, using p as an independent variable, as follows:

$$L^D n(L, X) = \alpha\exp(-p) \tag{12}$$

$$X/L^k = \beta p \tag{13}$$

However, although these equations can be fitted to the data over a wide range of amplitudes if the data are monofractal, in the multifractal model they can be fitted only over limited ranges of amplitude, as defined by ranges of p. Over each such limited range, Eqs. (12) and (13) can be fitted locally, but D, k, α, and β now all become functions of p (as defined by its value at the center of the respective range).

Thus, assuming the exponential form for the cumulative distribution of measured excess rates $n(L, X)$ over each such local amplitude range, centered on a prescribed value of p, multifractal scale invariance of $\overline{\Delta u}(y, L)$ implies that, for different values of the scale L, the relationship between $n(L, X)$ and X can be expressed in terms of the scaling equations

$$L^{D(p)} n(L, X) = \alpha(p)\exp(-p) \tag{14}$$

$$X/L^{k(p)} = \beta(p)p \tag{15}$$

In terms of a log-linear plot, the result of scaling is that line segments corresponding to the local fitting of the exponential model are translated vertically, by the factor $L^{D(p)}$, and rotated, by the factor $L^{k(p)}$, to lie, as illustrated schematically in Fig. 3b, on a segment of a scale-independent line defined by intercept $\log[\alpha(p)]$ and slope $[-1/\beta(p)]$. Examples of the collapse of curves, as illustrated in Fig. 3b, to segments of common straight lines over local ranges of amplitude, parameterized by p, are illustrated for measured data in Fig. 4. Repeating the process for a sequence of values of p, scaling exponents D and k are obtained as functions of p.

IV. Application to Low-Altitude Turbulence Data

A. Data Selection and Preprocessing

In the following, the method of data analysis is applied to measurements from a specially instrumented Gnat trainer aircraft flying at altitudes between approximately 1000 and 250 ft (300 and 75 m) over a variety of types of terrain. The turbulence measurement program[35,36] resulted in a total of approximately 400 runs, in the form of segments of flight records covering periods from 60 to 90 s. A wide range of wind conditions and conditions of terrain roughness was covered.

The three measured components of turbulence are referenced with respect to an aircraft body axis system, and are denoted by u_g (head), v_g (side), and w_g (normal). Although they are not components in Earth axes, in practice the restriction to a straight track, the fairly small pitch attitudes reached in the turbulence-measuring runs and the pilot's efforts to keep the wings level mean that the normal component, w_g, is very nearly the same as the vertical component. The x direction, in body axes, is along the aircraft forward path and the turbulence field is traversed at the aircraft flight speed, typically 180 m/s. Although the turbulence fluctuations are measured as functions of time, for analysis purposes they are converted to functions of position in space, assuming the standard frozen-field (Taylor) hypothesis and using the mean aircraft forward speed for the run in question.

To provide one basis for the classification of the measured turbulence time histories, power-spectral densities of individual turbulence components were measured. Typical examples are shown in Fig. 5, where measured power-spectral densities for the two horizontal components of turbulence velocity from one particular run are illustrated, plotted on log–log axes. The two components are respectively u_g (head-on), based on data from a miniature pitot sensor, and v_g (lateral), based on data from a Conrad yawmeter.

Two types of analysis have been used to estimate the power-spectral densities. The continuous curves in Fig. 5 correspond to estimates from a fast Fourier transform algorithm. The discrete symbols, at octave separation, correspond to broadband spectral estimates derived from a bandpass filter based on the smoothed-difference function, Eq. (2). This method has the advantage of allowing the spectral estimates to be associated with the differencing interval L used in the calculation of velocity increments, using the relationship (wavenumber)$^{-1}$ = wavelength = $2L$. Straight lines have been fitted, in Fig. 5, to four broadband estimates at octave intervals over the range indicated on the horizontal axis, limited at large wavenumbers by instrument cutoff. In terms of frequency, the fitted range is from 2 to 16 Hz. The wavenumber range depends on the flight speed but typically corresponds to wavelengths between 100 and 10 m. The slopes of the straight lines fitted to the measured data illustrated in Fig. 5 confirm that, for this particular run, the power-spectral densities of the horizontal components both follow a (wavenumber)$^{-\frac{5}{3}}$ power law, consistent with the classical theory (Kolmogorov[8]) for the inertial range. Departures of the spectral estimates from the fitted lines at small wave numbers (as in Fig. 5) allow the limit of the inertial range to be estimated. These indicate that the

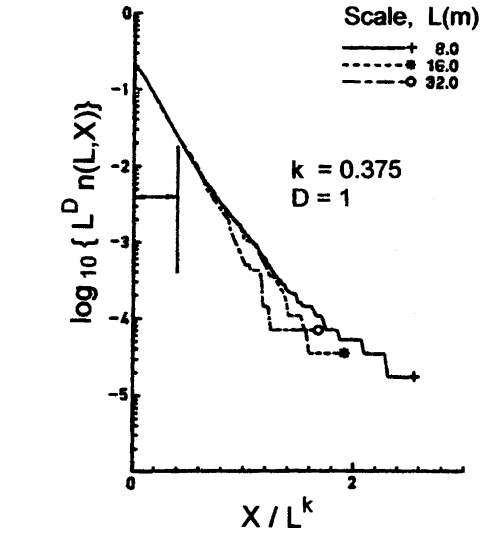

a)

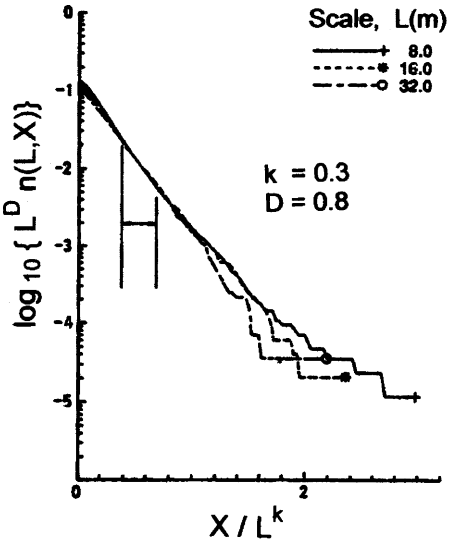

b)

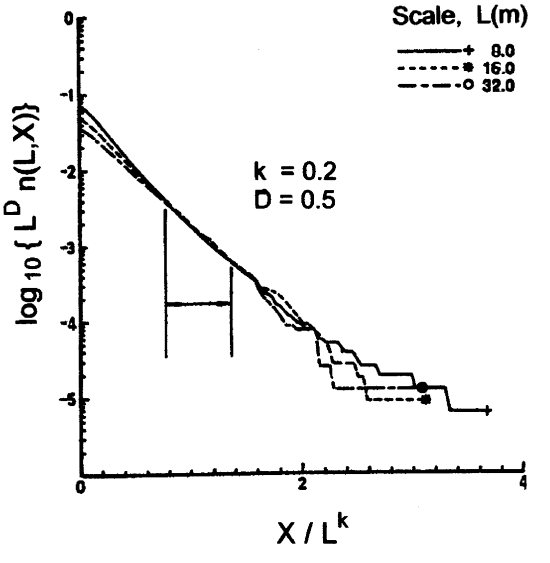

c)

Fig. 4 Amplitude ranges exhibiting scale invariance, corresponding to scaling exponents a) $k = 0.375$, $D = 1$; b) $k = 0.30$, $D = 0.8$; and c) $k = 0.20$, $D = 0.5$. High-intermittency block (H). Lateral component of turbulence velocity.

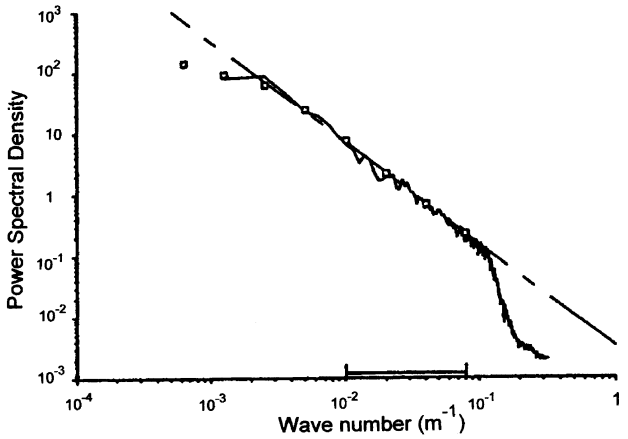

a)

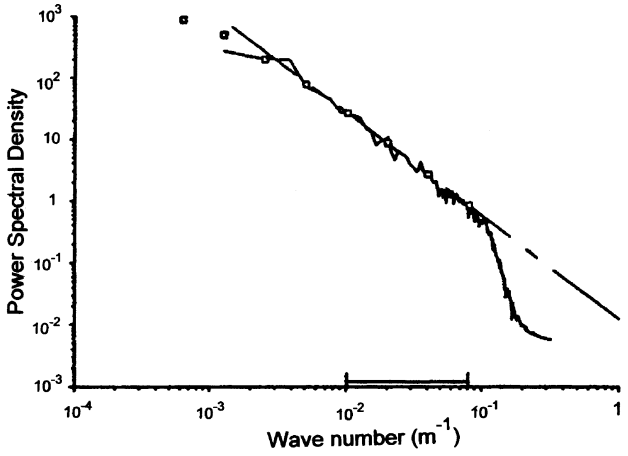

b)

Fig. 5 Examples of power-spectral densities for the two measured horizontal components of turbulence velocity from one particular run: a) u_g (head-on) component and b) v_g (side or lateral) component. The discrete symbols represent broadband estimates. Their departure from the $(-\frac{5}{3})$ line allows the limit of the inertial range to be estimated.

limit of the inertial range was in some cases being approached at a wavelength of 128 m (differencing interval $L = 64$ m). Although there is considerable scatter in the estimates of this limit, there is evidence[37] that it increases with altitude. For the lateral component, the mean value of this limit for flights over the smoother terrains is approximately equal to the altitude. Over the rougher terrains it tends to be somewhat larger.

Although measurements from the vertical component of turbulence were used for purposes of data classification (see later), over the range of scales for which it was possible to measure scaling exponents, the associated measured spectral exponents exhibited departures from the value of $(-\frac{5}{3})$, which effectively disqualified this component as adequately representative of inertial-range turbulence. Measured scaling exponents are thus presented subsequently (Sec. IV.B) for the lateral component only.

For purposes of statistical analysis, measurements from runs with similar properties have been merged to form data blocks within each of which the variability is constrained. A compromise had to be made in that it was desired to make the data blocks as large as possible, in order to improve statistical reliability, while at the same time restricting the variability within each block. Specifically, within each chosen block: 1) the measured power-spectral exponent for the lateral component is close to $(-\frac{5}{3})$; 2) the measured power-spectral exponent corresponding to the normal (vertical) component also lies within a limited range [but not necessarily close to $(-\frac{5}{3})$]; 3) the average intensities of the runs, as measured by the parameter β, Eq. (4), fitted over a range of amplitudes of between one and four standard deviations of the smoothed difference function $\overline{\Delta u}(y, L)$, Eq. (2), are similar; and 4) the runs are also similar in terms of

the parameter α, Eq. (4), again fitted over a range of amplitudes of between one and four standard deviations of the smoothed difference function $\overline{\Delta u}(y, L)$.

The dimensionless constant α has the property that α/L is the average population density, at scale L, of fluctuations in the smoothed difference function $\overline{\Delta u}(y, L)$. Reference 35 illustrates turbulence measurement runs with small values of α, which exhibit regions of relative quiescence punctuated intermittently by sudden severe fluctuations, and runs with large values of α, which are of a very regular or continuous nature. α may thus be regarded as an inverse measure of average intermittency. Three blocks of data were created, corresponding, respectively, to low (L), medium (M), and high (H) levels of average intermittency.

Because the mean aircraft speed varies from run to run, the sampling interval of the measured data, which corresponds to a fixed time increment, does not transform to a fixed distance in space. In order to achieve a common spatial sampling interval for runs within a data block the measured turbulence components were resampled to a fixed interval in space. Studies to choose an appropriate resampling rate showed that the shortest spatial sampling interval that could be achieved without degrading the quality of the measurements was 2 m. The smallest differencing interval L included in the study of two-point differences, which correspond to four sampling intervals, is thus 8 m for the resampled data (although values as small as 5 m were obtained for some individual unresampled runs where the aircraft speed was low).

The largest differencing interval L included in the study of two-point differences was constrained such that, for the lateral component of turbulence velocity, the associated broadband spectral estimate remained close to the $(-\frac{5}{3})$ fitted line (Fig. 5). As already indicated, departures below this line sometimes occurred at a wavelength of 128 m ($L = 64$ m). For the purpose of extracting reliable scaling exponents, the analysis of resampled data was thus restricted to values of L of 8, 16, and 32 m.

B. Results for the Lateral Component

In the case of the lateral component of turbulence velocity, the power-spectral density for each selected run followed the $(-\frac{5}{3})$ scaling law closely over the range of scales to which the following analysis was applied. For all three data blocks, described in Sec. IV.A, the scaling exponents k and D derived from measured absolute values of velocity increments decrease monotonically (Fig. 6) with increasing values of the moment parameter p (Sec. III). The greatest variations in the scaling exponents k and D are exhibited by the high-intermittency block (Fig. 6c), where, with increasing p, k decreases from 0.375 to approximately 0.2 and D reduces from 1 [$\boldsymbol{D} = 3$; Eq. (3)] to approximately 0.5 ($\boldsymbol{D} = 2.5$). Such variation is consistent with values that have been derived previously from measurements of structure-function exponents,[7,18] as described in Sec. II.C. Similar trends are exhibited by the data in blocks M and L. Each plot in Fig. 6 contains a data point corresponding to the classical Kolmogorov[8] theoretical value for the scaling exponents: $k = \frac{1}{3}$ and $D = 1$. Particularly in the case of the high-intermittency block, this point can be seen to be offset from the measured (k, D) curve. In this, and with respect to the overall trend in the (D, k) relationship, there is good qualitative agreement with the theoretical model of She and Leveque[28] (Fig. 2). It should be noted, however, that the results in Fig. 6 apply to transverse (lateral) velocity increments, whereas the theoretical model illustrated in Fig. 2 is applicable to homogeneous and isotropic turbulence and, moreover, was derived for longitudinal velocity increments (Sec. II.C).

For the high-intermittency block (H), Fig. 4 illustrates ranges of fluctuation amplitude over which particular pairs of scaling exponents (k, D) determine approximate scale invariance. Results correspond to increment intervals $L = 8$, 16, and 32 m. In Fig. 4a the scaling indices $k = 0.375$, $D = 1$, corresponding to low intensity ($p = 0$) in Fig. 6c, have been used in a plot of $\log [L^D n(L, X)]$ against X/L^k. It can be seen that the measured cumulative distributions collapse locally very well to a universal curve, demonstrating scale invariance, at the lowest amplitudes but fan out at higher amplitudes.

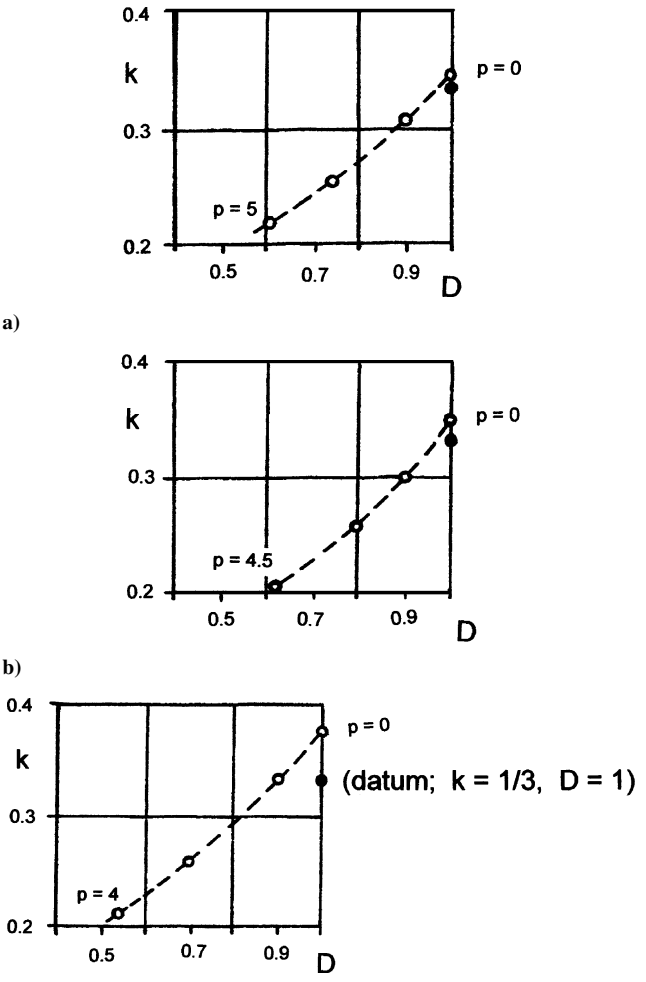

Fig. 6 Measured scaling exponents D and k from absolute values of velocity increments in measured lateral component of turbulence: a) low (L)-, b) medium (M)-, and c) high (H)-intermittency blocks. The isolated data points (k = 1/3, D = 1) correspond to the scaling in Kolmogorov's K41 theory, which is also the scaling implicit for the inertial range in the PSD statistical method of gust-load prediction.

In contrast, Figs. 4b and 4c show the same cumulative distributions scaled using exponents $k = 0.3$, $D = 0.8$ and $k = 0.2$, $D = 0.5$, respectively. It can be seen that, as k and D are reduced, following the trend with increasing p shown in Fig. 6c, the range of approximate scale invariance moves to higher amplitudes.

Although the results illustrated in Fig. 6 relate to measured severe turbulence, the levels of intensity encountered were still well below those that cause the structural loads to approach the levels that aircraft are designed to withstand. To estimate an appropriate value of the scaling exponent k for use in design criteria it is necessary to extrapolate to lower levels of probability, and thus to larger values of the parameter p. Although such extrapolation is an uncertain process, it is reasonable, on the basis of the experimental results in Fig. 6, to constrain the design-level value of k to the range 0.2 to 0.1, the value $k = \frac{1}{6}$ being a reasonable compromise. It should be noted that a value of $k = \frac{1}{6}$ has been proposed previously[6] as appropriate for representing severe-to-extreme gusts. Some implications of such a choice are evaluated in Sec. VI.

V. Multifractal Statistical-Discrete-Gust Model

In the following, starting from an existing monofractal version of the statistical-discrete-gust (SDG) model, described in Ref. 6, it is shown how the measured scaling exponents $D(p)$ and $k(p)$ may be incorporated into a method for estimating the associated turbulence-induced aircraft loads.

A. Monofractal Model

In the monofractal SDG model,[6] localized wind fluctuations in the inertial range are represented as ramp-shaped velocity increments (ramp gusts), embedded in regions either of constant velocity or of gradual decay over distances on the order of the inertial scale. Following the format of traditional turbulence models used for the prediction of aircraft loads[1–3] and prescribed in the current mandatory airworthiness requirements,[38] the model is one-dimensional. For instance, for the estimation of normal acceleration at the aircraft center of gravity (c.g.), and related structural loads associated with wing bending, only fluctuations in the vertical component of turbulence along the direction of the flight path are taken into account, this component being assumed to be constant in the transverse direction across the wing span. An analogous assumption is made with respect to the lateral component of turbulence, for the purpose of calculating fin loads. In terms of three-dimensional structures, it is in effect assumed that the velocity increments having the most relevance to structural loads arise as penetrations of shear layers, or sheets, whose thickness is on the order of the incremental distance, or gust-gradient distance, and where the axis of penetration is close to normal to the sheet.

The statistical model comprises an ensemble of such ramp gusts, covering a range of ramp lengths, or gradient distances, H, and having associated amplitudes, that is, two-point velocity differences, w. In its general form[6] the model is formulated to take account of both individual ramp gusts and of patterns comprising clustered sequences of such ramps; however, in this paper only the former case is considered. This is sufficient for predicting the response of well-damped systems whose response to an isolated ramp contains just a single peak of significant amplitude. It is relevant to the data-analysis method described in Sec. III that the requirement to have just a single peak of significant amplitude is satisfied by the output of the system defined by the data-processing filter, $\overline{\Delta u}(y, L)$, Eq. (2).

For any system, such as an aircraft load or the data-processing filter $\overline{\Delta u}(y, L)$, a response function $\gamma(H)$ is defined[6] to be the magnitude of the maximum peak response to a ramp gust of gradient distance H and amplitude $w = H^k$, where k is the prescribed (monofractal) velocity-difference scaling exponent. By varying H, the tuned gradient distance $H = \bar{H}$ corresponding to a stationary maximum value $\gamma(\bar{H})$ (the tuned response) is obtained. In the monofractal model it is further assumed that, for any given value of ramp length H, the probability distribution for w takes the form of an exponential.

Thus, assuming the ensemble of ramp gusts to be characterized by a single fractal dimension D in association with the scaling exponent k (Sec. II.B), the average rate of occurrence $n(X)$ of system response peaks greater than or equal to X is given[6] by

$$n(X) = \int_0^{H_{\max}} \frac{a(H)}{H^2} \exp\left[-\frac{X}{b\gamma(H)}\right] \mathrm{d}H \tag{16}$$

where $a(H) \approx H^{1-D}$. Applying Laplace's asymptotic method, the integral in Eq. (16) may be evaluated approximately to give[6]

$$(\bar{H})^D n(X) = \alpha \exp[-X/\beta\gamma(\bar{H})] \tag{17}$$

To expose the scaling relationships inherent in Eq. (17) more clearly, we introduce a first-order approximation that neglects the change in the tuned gradient distance $\bar{H}$ that in general occurs when the scaling exponent k is varied, simply rescaling the amplitude of the tuned gust pattern and the amplitude of the associated response. Equation (17) then takes the approximate form

$$(\bar{H}_0)^D n(X) = \alpha \exp\left\{-X\Big/\left[\beta \cdot (\bar{H}_0)^{k-\frac{1}{3}} \gamma_0(\bar{H}_0)\right]\right\} \tag{18}$$

where $\bar{H}_0$ and γ_0 refer to a datum case evaluated for the Kolmogorov model with $D = 1$ and $k = \frac{1}{3}$. In the case where the system is the smoothing-and-differencing filter introduced in Sec. II.B, Eq. (18) may be identified with Eq. (4), where $\bar{H}_0 = L$ and $\gamma_0(\bar{H}_0) = L^{\frac{1}{3}}$.

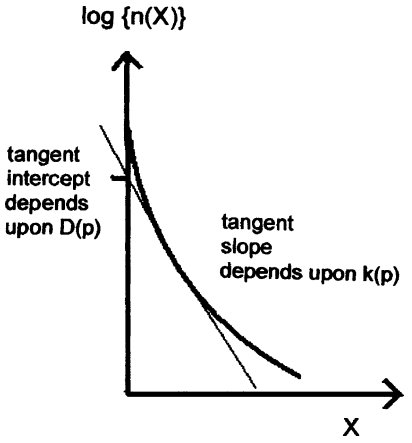

Fig. 7 Multifractal SDG model for system response based on Eq. (19). Each tangent, which corresponds to a monofractal component parameterized by p, is specified by its slope $k(p)$ and intercept determined by $D(p)$. Compare Fig. 1.

B. Multifractal Model

The monofractal SDG model, as outlined above, employs a particular pair of scaling exponents k, D, which are chosen according to the fluctuation intensity that it is required to represent. In particular, $k = \frac{1}{3}$ has been recommended previously[6] as a practicable value for predicting aircraft response in turbulence of low to average intensity, whereas a value of $k = \frac{1}{6}$ has been proposed[6] as more appropriate for representing the more extreme gusts. These values may be seen to be consistent with the results of measurements described in Sec. IV. The multifractal formulation of the SDG model, on the other hand, comprises a collection of monofractal models, parameterized in the form $k(p)$, $D(p)$ by the moment-order variable p, which represents "intensity." It thus takes into account all fluctuation intensities from low amplitude to extreme, and hence all scaling exponents k in the range $\frac{1}{3}$ to $\frac{1}{6}$ (or even lower values).

Equation (18) is then applied separately to each monofractal component of the model, where now α, β, k, and D are all functions of p:

$$(\bar{H}_0)^{D(p)} n(X) = \alpha(p) \exp\left\{-X\Big/\left[\beta(p) \cdot (\bar{H}_0)^{k(p)-\frac{1}{3}} \gamma_0(\bar{H}_0)\right]\right\} \tag{19}$$

In this paper it has been shown (Secs. III and IV), how such a multifractal representation can be fitted to measured data and Fig. 6 shows examples of the measured functions $k(p)$ and $D(p)$. Also measured (but not illustrated) were the functions $\alpha(p)$ and $\beta(p)$. It may be noted that the functions $\alpha(p)$ and $\beta(p)$ define the shape of a datum distribution corresponding to the particular scale $(\bar{H}_0) = 1$.

For any chosen value of p, corresponding to a particular monofractal model having an exponential distribution, a plot of Eq. (19) using log-linear axes {i.e., $\log[n(X)]$ against X} results in a straight line (Fig. 7) whose intercept with the vertical axis depends upon D and whose slope depends on k. Variation of p leads to a family of such lines whose envelope, having the shape of a stretched exponential, represents the distribution of excess, $n(X)$, for the multifractal SDG model for system response.

For practical applications of the multifractal SDG model to calculate system response, it is sufficient to approximate the envelope $n(X)$ (Fig. 7) by just a limited number of tangents specified by associated values of p. For any value of X, each monofractal component, Eq. (19), is evaluated and the maximum of the resulting values of $n(x)$ is then the output of the multifractal model.

C. Relationship to Structure Functions

As described in Sec. II.C, the multifractal model of turbulence may be related to the structure-function exponent ζ_p, where p is the moment-order parameter. Indeed, the multifractal scaling exponents $k(p)$ and $D(p)$ have in the past usually been derived by first measuring the function ζ_p and then using further data processing based on relationships illustrated in Fig. 1. As illustrated in Fig. 1, ζ_p may be defined as an envelope of tangents, exactly as is the case

for $n(X)$ (Fig. 7). For any specified value of p, say $\bar{p}$, the associated tangent is given[7] by the linear equation

$$\zeta_p = pk(\bar{p}) + 1 - D(\bar{p}) \tag{20}$$

Given the multifractal scaling exponents $k(p)$ and $D(p)$, just as the multifractal system-response distribution $n(X)$ (Fig. 7) can be generated as an envelope of tangents given by Eq. (19), so the multifractal structure-function exponent ζ_p (Fig. 1) can be generated as an envelope of tangents given by Eq. (20). In each case the slope of the tangent is determined by k and the intercept is determined by D. It can be seen from the analysis based on Eqs. (19) and (20) that the scaling exponents $k(p)$ and $D(p)$ provide a one-to-one mapping between the two sets of tangents illustrated in Figs. 1 and 7 and hence between ζ_p and $n(X)$.

In the situation where the system is the data-processing filter defined, for a particular value of L, by Eq. (2), the tangent shown in Fig. 7 may be identified with the common tangent to the curves, representing a range of values of L, in Fig. 3b. In Fig. 3b the effects of $k(p)$ and $D(p)$ on the tangent slope and intercept, illustrated in Fig. 7, have been absorbed by the respective scaling of the $n(X)$ and X axes.

VI. Relevance of Results to Existing Models for Predicting Aircraft Loads

The earliest reference in the aeronautical literature to the properties of turbulence in the inertial range discussed in this paper, and their relevance to the statistics of aircraft response, is that of Chen.[4] Chen used four independent data sources: High Altitude Clear Air Turbulence (HICAT), Severe Storm Turbulence (SEST), Barbados Oceanographic and Meteorological Experiment (BOMEX), and Wind Tunnel Turbulence (WITT). In all four cases the probability distribution of velocity increments showed the characteristic stretched exponential form, with kurtosis significantly greater than that of a Gaussian distribution. Chen[4] went on to use these results to highlight the limitations of the traditional statistical approach to the prediction of aircraft dynamic loads in atmospheric turbulence,[1–3] the power-spectral-density (PSD) method. For application to the inertial range, this method is based mathematically[1] on the simplifying assumption that, at least over patches of limited extent, turbulence can be represented as a stationary Gaussian process having a power-spectral density that follows the classical $(-\frac{5}{3})$ power law and velocity increments that follow a $(\frac{1}{3})$ scaling law. Although it is now widely accepted that turbulence velocity is in fact a non-Gaussian process, the method continues to be used, in particular for relating the loads on one aircraft to the loads on another with differing dynamic response, and for relating the loads at different stations on the same aircraft.

The non-Gaussian structure exhibited by measured turbulence-velocity records influences aircraft loads primarily via the statistics of velocity increments. As illustrated by Chen,[4] and confirmed by the results presented in this paper, turbulence-velocity increments have strong-tailed probability distributions of exponential, rather than Gaussian, form. The tails of these exponential-type distributions stand out well beyond the tails of a Gaussian distribution, resulting in much higher predicted probabilities of events at, for example, five or six times the root-mean-square (rms) amplitude. This property does not in itself necessarily produce errors in the PSD method of load prediction, as it has been shown[1] that exponential tails can be reproduced by the expedient of modeling turbulence as a sequence of Gaussian patches whose rms itself follows a specified distribution. In the past, this result has sometimes been quoted[2] as a means by which the PSD method can deal with the non-Gaussian structure of turbulence. However, the more significant aspect of non-Gaussian turbulence which influences aircraft response predictions is not that the tails of the distributions of velocity increments are exponential but rather that the strengths of the tails vary with gradient distance, the strength increasing as gradient distance is reduced. As a result, for small values of the gradient distance H the PSD method, in which the shape of the distribution is assumed to be independent of H, tends to underestimate the magnitude of velocity increments at the tails of the distribution, whereas for large values of H it tends to overestimate them. In turn, this influences aircraft loads via related response modes which tune to different values of H. Specifically, loads predicted by the PSD method that depend on response modes that tune to large gradient distances tend to be conservative. Conversely, loads that depend on response modes that tune to short gradient distances tend to be underestimated.

Quantitatively, these trends result from the fact that whereas the PSD method assumes implicitly that the amplitudes of velocity increments in the inertial range scale like "one-third," for the more severe turbulence fluctuations the increasing strengths of the tails on the distributions, with reducing scale, imply a scaling exponent k of less than one-third.

A simple response quantity that can be used to illustrate the effect of the scaling exponent k is Δn, the normal acceleration at the c.g. Under the simplifying assumption that the aircraft is constrained to respond in vertical translation only, with no pitching, it is shown in Ref. 20 that, in response to vertical gusts, Δn is proportional to $V/[(W/S)/\rho g a]^{1-k}$, where W/S is the wing loading, a is the lift-curve slope, ρ is air density, and g is acceleration due to gravity. Suppose now that two gust models, one with a value of the scaling exponent k equal to one-sixth (representing non-Gaussian severe turbulence) and the other with k equal to one-third (representing Gaussian turbulence, as in the PSD method) are matched in overall intensity to give equal magnitudes of Δn for some aircraft with intermediate wing loading W/S. Then, if we consider a family of aircraft with differing wing loadings, it follows from the preceding scaling expression for Δn that, relative to the non-Gaussian model of severe turbulence, the PSD method will predict conservative values of Δn for those aircraft, such as heavy jet transports, with large values of W/S and, conversely, will tend to underestimate Δn for light aircraft with small values of W/S. Moreover, this result has direct implications for structural loads because, for example, root-wing-bending loads due to vertical gusts follow closely the trends in the response in normal acceleration at the c.g.

A further example of the practical effect of employing a gust model that incorporates non-Gaussian scaling of large-amplitude fluctuations in severe turbulence has been described in Ref. 39. Here, for a particular class of (turboprop) aircraft, lateral gust loads on the tail (such as fin bending), which depend dynamically on response in the relatively low-frequency Dutch-roll mode and hence on increments in the lateral component of gust velocity over relatively long gradient distances, are compared with vertical gust loads on the wing (such as wing bending), which typically depend on increments in the vertical component of gust velocity over shorter gradient distances. Following the standard assumption, made in the airworthiness requirements,[38] that the vertical and lateral components of turbulence follow the same statistics in the inertial range, it is shown in Ref. 39 that, when calculated using a monofractal SDG model (Sec. V.A) that incorporates a $k = \frac{1}{6}$ scaling law for velocity increments, the ratios of these loads are typically smaller than the ratios calculated by the PSD method (which implicitly uses a $k = \frac{1}{3}$ law). Thus, as compared with the results of a PSD analysis, a loads prediction based on a monofractal SDG model of severe turbulence with $k = \frac{1}{6}$ leads to a redistribution of the magnitudes of predicted responses to vertical and lateral gusts.[39] This in turn would lead to an associated redistribution of aircraft strength/weight between the wing and the tail to achieve equal margins of safety in each axis.

To take account of the more extreme, and relatively isolated, atmospheric disturbances, the current airworthiness requirements for aircraft loads[38] do incorporate, in addition to the PSD statistical model, a deterministic tuned-discrete-gust model defined in terms of a specified family of velocity profiles of one-minus-cosine form in which an up-ramp, whose amplitude is proportional to gradient distance to the power $\frac{1}{6}$, is followed, with zero spacing, by a down-ramp of equal amplitude and gradient distance. This use of a one-sixth scaling law to represent fluctuations of high intensity is compatible with the measured statistics of turbulence-velocity increments presented in this paper (Sec. IV). The deterministic tuned-discrete-gust model in the airworthiness requirements may thus be interpreted statistically as a particular implementation of the monofractal SDG model described in Sec. V, corresponding to a fixed, and relatively

large, value of the moment-order parameter p (albeit having as elementary components coupled pairs of up–down ramps, rather than single isolated ramps).

VII. Conclusions

This paper has presented an analysis of atmospheric turbulence in the inertial range, at scales relevant to aircraft response, using data obtained from flights at low altitudes by a specially-instrumented aircraft. Non-Gaussian statistical properties of the measured turbulence have been demonstrated, using a new method of data analysis based on the scaling of probability distributions, and the results shown to be consistent with those from previous experiments, made at smaller scales, and with current theoretical understanding of the structure of inertial-range turbulence.[7] It has been demonstrated how the results have direct implications for aircraft loads prediction.

The non-Gaussian characteristics have been expressed in terms of probability distributions of absolute values of two-point velocity differences, which have been confirmed to have tails of broadly exponential type (stretched exponentials), where the strength of the tail increases as scale is reduced. This phenomenon has been quantified in terms of exponents $k(p)$ and $D(p)$, where k defines the scaling of the amplitude of velocity differences, D is a fractal dimension that describes "space-fillingness," and p is a moment-order parameter that is a measure of fluctuation intensity. The measured variations in these exponents with p (Fig. 6) follow a trend familiar from the results of previous measurements,[7] obtained by a different method of analysis based on the scaling of structure-function exponents, and are broadly consistent with the predictions (Fig. 2) of a particular theoretical model. Specifically, the measured exponent k reduces from a value of rather greater than $\frac{1}{3}$ at the lowest intensities (smallest values of p) to a value close to 0.2 at the highest intensities (largest values of p) at which reliable estimates could be made. It has been concluded that, at the severe-to-extreme intensities that influence aircraft safety, k can with some confidence be assumed to lie in the extrapolated range 0.2 to 0.1, with the value of $\frac{1}{6}$ being a reasonable compromise. These results are contrasted in Fig. 6 with the scaling in Kolmogorov's K41 theory,[8] which is also the scaling implicit in the PSD statistical method of gust-loads prediction.[1–3]

It has been demonstrated how the exponents $k(p)$ and $D(p)$ can be incorporated into a multifractal formulation of the statistical-discrete-gust (SDG) method for predicting aircraft response, based on a previous monofractal model.[6] By this means it has been possible to demonstrate the manner in which the non-Gaussian statistics of inertial-range turbulence, quantified in terms of these exponents, influence aircraft loads prediction. Differences between the resulting estimated loads and loads predicted by the statistical method prescribed in the current mandatory requirements,[38] the PSD method which is based on Gaussian statistics, have been identified. Specifically, for aircraft response modes that tune to large gradient distances, it has been concluded that in comparison with the loads predicted by the non-Gaussian SDG model of severe-to-extreme turbulence, loads predicted by the PSD method will tend to be conservative. Conversely, loads that depend on response modes that tune to short gradient distances will tend to be underestimated.

Implications for the effects of non-Gaussian statistics on the relationships between root-wing-bending loads on aircraft having differing wing loadings, or lift-curve slopes, and between wing loads (due to vertical gusts) and tail loads (due to lateral gusts) on the same aircraft, have been discussed. In the latter case, assuming (as in the current mandatory requirements[38]) vertical and lateral gusts to follow the same statistics, the adoption of a criterion which takes account of the demonstrated non-Gaussian scaling of velocity increments could lead to a redistribution of weight/strength between the wing and the tail in order to achieve balanced safety margins with respect to vertical and lateral gusts.

VIII. Appendix: Parametric Form for Excess Rate

Under the assumption that, over limited ranges of amplitude X, the measured number, per unit distance y, of local extrema in $\overline{\Delta u}(y, L)$ having magnitude greater than X, can be approximated by the exponential form

$$n(X) = a \exp(-X/b) \tag{A1}$$

where a and b are functions of L, the associated probability density of local extrema is proportional to $-n'(X) = (a/b)\exp(-X/b)$. Thus, in the terminology of Eq. (8), $f(X) = A \cdot \exp(-X/b)$, where A is a normalizing constant. Application of Eq. (8) thus gives $X_p = pb$, and substitution into Eq. (9) gives $n(X_p) = a \exp(-p)$. Replacing X_p simply by X gives Eqs. (10) and (11).

References

[1] Hoblit, F. M., *Gust Loads on Aircraft: Concepts and Applications*, AIAA Education Series, AIAA, Washington, DC, 1988, Chap. 4.

[2] Houbolt, J. C., "Atmospheric Turbulence," *AIAA Journal*, Vol. 11, No. 4, 1973, pp. 421–437.

[3] Etkin, B., "Turbulent Wind and its Effect on Flight," *Journal of Aircraft*, Vol. 18, No. 5, 1981, pp. 327–345.

[4] Chen, W-Y., "Application of Rice's Exceedance Statistics to Atmospheric Turbulence," *AIAA Journal*, Vol. 10, No. 8, 1972, pp. 1103–1105.

[5] Rice, S. O., "Mathematical Analysis of Random Noise," *Bell System Technical Journal*, Vol. 23, No. 3, 1944, pp. 282–332; Vol. 24, No. 1, 1945, pp. 46–156.

[6] Jones, J. G., "Statistical Discrete Gust Method for Predicting Aircraft Loads and Dynamic Response," *Journal of Aircraft*, Vol. 26, No. 4, 1989, pp. 382–392.

[7] Frisch, U., *Turbulence, the Legacy of A. N. Kolmogorov*, Cambridge Univ. Press, Cambridge, England, U.K., 1995.

[8] Kolmogorov, A. N., "The Local Structure of Turbulence in Incompressible Viscous Fluid for Very Large Reynolds Number," *Comptes Rendus (Doklady) de l'Academie des Sciences de l'URSS*, Vol. 30, No. 4, 1941, pp. 301–305; reprinted in *Proceedings of the Royal Society of London, Series A: Mathematical and Physical Sciences*, Vol. 434, No. 1890, 1991, pp. 9–13.

[9] Kolmogorov, A. N., "A Refinement of Previous Hypotheses Concerning the Local Structure of Turbulence in a Viscous Incompressible Fluid at High Reynolds Number," *Journal of Fluid Mechanics*, Vol. 13, 1962, pp. 82–85.

[10] Obukhov, A. M., "Some Specific Features of Atmospheric Turbulence," *Journal of Fluid Mechanics*, Vol. 13, 1962, pp. 77–81.

[11] Van Atta, C. W., and Chen, W. Y., "Structure Functions of Turbulence in the Atmospheric Boundary Layer Over the Ocean," *Journal of Fluid Mechanics*, Vol. 44, 1970, pp. 145–159.

[12] Van Atta, C. W., and Park, J., "Statistical Self-Similarity and Inertial Subrange Turbulence," *Statistical Models and Turbulence*, Lecture Notes in Physics 12, edited by M. Rosenblatt and C. W. Van Atta, Springer-Verlag, Berlin, 1972, pp. 402–426.

[13] Mandelbrot, B. B., "Intermittent Turbulence in Self-Similar Cascades: Divergence of High Moments and Dimensions of the Carrier," *Journal of Fluid Mechanics*, Vol. 62, 1974, pp. 331–358.

[14] Frisch, U., Sulem, P.-L., and Nelkin, M., "A Simple Dynamical Model of Intermittent Fully Developed Turbulence," *Journal of Fluid Mechanics*, Vol. 87, pt. 4, 1978, pp. 719–736.

[15] Parisi, G., and Frisch, U., "On the Singularity Structure of Fully Developed Turbulence," *Turbulence and Predictability in Geophysical Fluid Dynamics*, edited by M. Ghil, R. Benzi, and G. Parisi, North-Holland, Amsterdam, 1985, pp. 84–87.

[16] Benzi, R., Paladin, G., Parisi, G., and Vulpiani, A., "On the Multifractal Nature of Fully Developed Turbulence and Chaotic Systems," *Journal of Physics*, Vol. A17, No. 18, 1984, pp. 3521–3531.

[17] Meneveau, C., and Sreenivasan, K. R., "The Multifractal Spectrum of the Dissipation Field in Turbulent Flows," *Nuclear Physics B Proceedings Supplement*, Vol. 2, Nov. 1987, pp. 49–76.

[18] Meneveau, C., and Sreenivasan, K. R., "The Multifractal Nature of Turbulent Energy Dissipation," *Journal of Fluid Mechanics*, Vol. 224, 1991, pp. 429–484.

[19] She, Z., Jackson, E., and Orszag, S. A., "Structure and Dynamics of Homogeneous Turbulence: Models and Simulations," *Proceedings of the Royal Society of London, Series A: Mathematical and Physical Sciences*, Vol. 434, No. 1890, 1991, pp. 101–124.

[20] Jones, J. G., Foster, G. W., and Haynes, A., "Fractal Properties of Inertial Range Turbulence with Implications for Aircraft Response," *Aeronautical Journal of the Royal Aeronautical Society*, Vol. 92, Oct. 1988, pp. 301–308.

[21] Frederiksen, R. D., Dahm, W. J. A., and Dowling, D. R., "Experimental Assessment of Fractal Scale Similarity in Turbulent Flows. Part 2. Higher-Dimensional Intersections and Non-Fractal Inclusions," *Journal of Fluid Mechanics*, Vol. 338, 1997, pp. 89–126.

[22]Gagne, Y., Hopfinger, E., and Frisch, U., "A New Universal Scaling for Fully Developed Turbulence: The Distribution of Velocity Increments," *New Trends in Nonlinear Dynamics and Pattern-Forming Phenomena*, edited by P. Coullet and P. Huerre, NATO ASI, Vol. 237, Plenum, New York, 1990, pp. 315–319.

[23]Gagne, Y., and Castaing, B., "A Universal Representation without Global Scaling Invariance of Energy Spectra in Developed Turbulence," *Comptes Rendus Academie des Sciences, Paris, Serie II*, Vol. 312, No. 5, 1991, pp. 441–445.

[24]Narasimha, R., "The Utility and Drawbacks of Traditional Approaches," *Whither Turbulence? Turbulence at the Crossroads*, edited by J. L. Lumley, No. 357, Lecture Notes in Physics, Springer-Verlag, Berlin, 1990, pp. 13–48.

[25]Jones, J. G., Foster, G. W., and Earwicker, P. G., "Wavelet Analysis of Gust Structure in Measured Atmospheric Turbulence Data," *Journal of Aircraft*, Vol. 30, No. 1, 1993, pp. 94–99.

[26]Anselmet, F., Gagne, Y., Hopfinger, E. J., and Antonia, R. A., "High-Order Velocity Structure Functions in Turbulent Shear Flow," *Journal of Fluid Mechanics*, Vol. 140, 1984, pp. 63–89.

[27]She, Z., and Orszag, S. A., "Physical Model of Intermittency in Turbulence: Inertial-Range Non-Gaussian Statistics," *Physics Review Letters*, Vol. 66, No. 13, 1991, pp. 1701–1704.

[28]She, Z., and Leveque, E., "Universal Scaling Laws in Fully Developed Turbulence," *Physical Review Letters*, Vol. 72, No. 3, 1994, pp. 336–339.

[29]Chen, S., Sreenivasan, K. R., Nelkin, M., and Cao, N., "Refined Similarity Hypothesis for Transverse Structure Functions in Fluid Turbulence," *Physical Review Letters*, Vol. 79, No. 12, 1997, pp. 2253–2256.

[30]Dhruva, B., Tsuji, Y., and Sreenivasan, K. R., "Transverse Structure Functions in High-Reynolds-Number Turbulence," *Physical Review E*, Vol. 56, No. 5, 1997, pp. R4928–R4930.

[31]Shen, X., and Warhaft, Z., "The Anisotropy of the Small Scale Structure in High Reynolds Number Turbulent Shear Flow," *Physics of Fluids*, Vol. 12, No. 11, 2000, pp. 2976–2989.

[32]Kurien, S., and Sreenivasan, K. R., "Measures of Anisotropy and the Universal Properties of Turbulence," *New Trends in Turbulence*, NATO Advanced Study Institute, Les Houches, Springer and EDP-Sciences, Berlin, 2001, pp. 53–111.

[33]Schumacher, J., Sreenivasan, K. R., and Yeung, P. K., "Derivative Moments in Turbulent Shear Flows," *Physics of Fluids*, Vol. 15, No. 1, 2003, pp. 84–90.

[34]Shraiman, B. I., and Siggia, E. D., "Scalar Turbulence," *Nature*, Vol. 405, No. 6787, 2000, pp. 639–646.

[35]Foster, G. W., and Jones, J. G., "Analysis of Atmospheric Turbulence Measurements by Spectral and Discrete-Gust Methods," *Aeronautical Journal of the Royal Aeronautical Society*, Vol. 93, No. 925, 1989, pp. 162–176.

[36]Foster, G. W., and Jones, J. G., "Measurement and Analysis of Low Altitude Atmospheric Turbulence," AGARD Rept. R-734, Paper 2, 1987.

[37]Foster, G. W., "Results of Low Altitude Atmospheric Turbulence Measurements," Royal Aircraft Establishment, TR-87015, Farnborough, England, U.K., Feb. 1987.

[38]Federal Aviation Regulations, "Part 25-86—Airworthiness Standards: Transport Category Airplanes," Federal Aviation Administration, U.S. Dept. of Transportation, Washington, DC, Nov. 1996.

[39]Glaser, J., "Reviewer Commentary," Documentation of the Linear Statistical Discrete Gust Method, Office of Aviation Research, Federal Aviation Administration, U.S. Dept. of Transportation, DOT/FAA/AR-04/20, Washington, DC, July 2004, Appendix F, pp. F1–F3.

W. Dahm
Associate Editor